PCCP

COMMUNICATION

Cite this: *Phys. Chem. Chem. Phys.*, 2017, **19**, 1731

Received 26th September 2016,
Accepted 12th December 2016

DOI: 10.1039/c6cp06602j

www.rsc.org/pccp

Modeling the abnormally slow infiltration rate in mesoporous films

Claudio L. A. Berli,*[a] Magalí Mercuri[b] and Martín G. Bellino[b]

Mesoporous films have been shown to exhibit striking behaviors in capillary-driven infiltration experiments. The process has been shown to follow classical Lucas–Washburn dynamics, but the effective pore radius has been calculated from hydrodynamic resistance considerations to be orders of magnitude lower than measured pore dimensions. In addition, the infiltration rate has been observed to decrease with increasing pore diameter, in contrast to the expected trend for capillary-like pores. Here, we present a simple model accounting for the mechanism behind these anomalous effects. We found the infiltration rate to be inversely proportional to the cubed ratio of pore to neck size. This physical scaling correctly modeled both the magnitude of the infiltration rate and its variation with pore diameters, for a wide range of experimental data. The model established a connection between capillary filling dynamics and nanoscale pore structure, which is of practical interest for the design and characterization of mesoporous films.

The versatile use of mesoporous films in microfluidic devices is opening up many new applications for these films, from biocatalyst films[1] to optical resonators.[2] Nevertheless, understanding flow and mass transport at the nanoscale requires further efforts, despite the intense research activity that has already taken place in the field.[3] Recently, the comprehensive experimental work of Ceratti *et al.*[4] revealed the critical effects of pore characteristics on capillary filling in mesoporous films and, at the same time, posed challenging questions about the relationship between nanoscale structure and macroscopic fluid dynamics. In the present work, we obtained theoretical evidence to explain the apparent contradiction between experimental values of infiltration rates and pore size data. For this purpose we took advantage of the detailed characterization of the wide variety of mesoporous films reported by Ceratti *et al.*[4]

[a] *INTEC (Universidad Nacional del Litoral-CONICET) Predio CCT CONICET Santa Fe, RN 168, 3000, Santa Fe, Argentina. E-mail: cberli@santafe-conicet.gov.ar*
[b] *Departamento de Micro y Nanotecnología, Comisión Nacional de Energía Atómica, Av. Gral. Paz 1499, San Martín, Buenos Aires, Argentina*

Capillary-driven infiltration in porous media follows classical Lucas–Washburn dynamics, *i.e.*, $l^2 = 2ct$, where l is the position of the imbibition front at time t, and c is a dynamic coefficient that depends on the characteristics of both the fluid and porous matrix.[5,6] This expression derives from the meniscus velocity equation $u(l) = c/l$, which is a consequence of the balance between the Laplace driving force and the viscous resistance in capillary tubes, provided evaporation is absent and gravity effects are negligible.[7] The simplest physical representation of the porous space is the well-known capillary bundle (CB) model, which was first proposed by Washburn,[6] and consists of straight capillaries, of radius r_{eff}, that are not interconnected, and that are aligned in the flow direction (Fig. 1a). For this ideal configuration,

$$c_{\mathrm{CB}} = \frac{\gamma \cos\theta r_{\mathrm{eff}}}{4\mu} \quad (1)$$

where μ is the fluid viscosity, γ is the surface tension, and θ is the meniscus contact angle. This equation establishes a connection between the pore-scale geometry and the measured variables in the imbibition experiments. The effective radius r_{eff} obtained from eqn (1) does not necessarily match the actual pore radius of the substrate, as it represents the equivalent capillary that produces the same infiltration rate. As expected, r_{eff} and pore size measured by microcopy, specifically scanning electron microscopy (SEM), coincide in the case of pores with large aspect ratios, such as those obtained by electrochemical etching in nanoporous silica[8] and alumina membranes.[9] In any case, eqn (1) gives a good measure of the characteristic size of the capillary at the pore level, and it is customarily employed to interpret capillary filling experiments in different porous substrates.

Even for mesoporous films prepared by combining sol–gel chemistry and supramolecular templates, capillary infiltration follows the relation $l^2 \sim t$, but the process is extremely slow. Consequently, an analysis of the experimental values of the dynamic coefficient c_{exp} that uses eqn (1) would yield anomalous values of r_{eff}, values that may be orders of magnitude lower than pore sizes measured by environmental ellipsometry porosimetry (EEP), or observed by SEM. For example, a c_{exp}

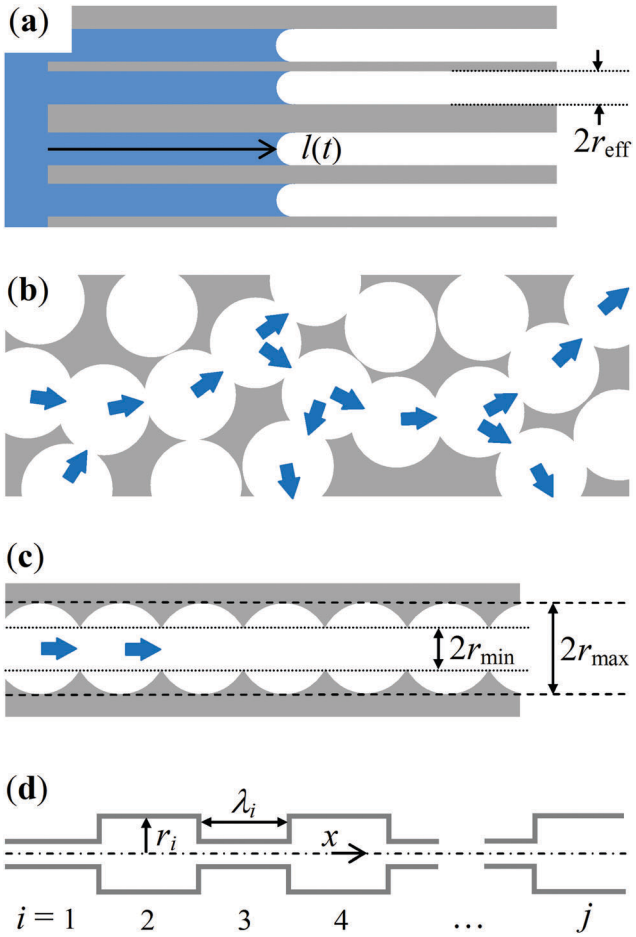

Fig. 1 Schematic representations of (a) the capillary bundle model, (b) mesoporous structures, where blue arrows indicate arbitrary flow paths during capillary-driven infiltration, (c) the concept of periodically constricted nanochannels, and (d) the geometry of the simplified stepped tube used in calculations.

value of 10^{-10} m^2 s^{-1}, which is typically found for the infiltration of water,[4] would yield an r_{eff} of about 0.02 nm according to eqn (1). This physically unrealistic value clearly indicates that there must be some topological feature controlling the fluid dynamics at the nanoscale.

A second controversial issue has arisen regarding these critical dimensions: c_{exp} has been found to systematically decrease with increasing pore diameter, for a rather constant neck size (Fig. 9b in ref. 4), in contradiction with the linear relation $c_{CB} \sim r_{eff}$ given by eqn (1). These striking results suggest the need for more insightful descriptions of the porous structure from the viewpoint of fluid dynamics.

Adsorption–desorption experiments using mesoporous films indicated the presence of relatively wide pores interconnected by small throats, or bottlenecks (Fig. 6 and 7 in ref. 4), the size of which can be measured by EEP (see Table 1 below). In this regard, we here derived a simple model capturing the essential feature of the problem, namely the presence of periodic changes in the cross-sectional area of the flow path, as shown schematically in Fig. 1b. By analogy to the CB model,

Table 1 Experimental pore size and infiltration rate values for different mesoporous film samples reported in ref. 4. The maximum ($2r_{max}$) and minimum ($2r_{min}$) pore diameter values were obtained from the adsorption–desorption EEP isotherms. $2c_{exp}$ values were obtained from the slopes of the infiltration curves l^2 *vs.* t

	Pore diameter (nm)		$2c_{exp} \times 10^{-2}$ (mm^2 s^{-1})	
Sample	$2r_{max}$	$2r_{min}$	Water	IL
PPN	17.1	15.2	7	1.2
Bj1	5.2	3.8	2.8	0.18
Bj2	4.6	3.4	2.1	0.02
Bj3	6.3	4.4	1.9	0.028
F1	6.2	3.4	1.4	—
F2	7.8	3.5	0.64	0.013
PBd1	12	2.3	0.21	—
PBd2	10.2	2	0.06	0.00017
PS7	17.5	3	0.044	—
PBd3	24.3	4.1	0.015	—

the mesoporous membrane was considered in our work to be an assembly of straight nanochannels, now with periodic variations of the pore radius (Fig. 1c). As a first approximation, a cylindrical tube with periodic step changes in its radius was considered here, as shown schematically in Fig. 1d. In the first segment ($0 \le x \le \lambda_1$), the meniscus velocity was calculated using the equation

$$u(l)_{i=1} = \frac{r_1^2 \Delta p_1}{8\mu l}, \tag{2}$$

which is the Lucas–Washburn prediction for uniform capillaries,[5,6] where $\Delta p_1 = 2\gamma \cos\theta / r_1$ is the Laplace driving pressure.[7] When the meniscus passes to the next segment, a step-wise variation of fluid velocity would take place, but mass continuity would impose an instantaneously equal flow rate. Thus for $\lambda_1 \le x \le \lambda_2$, the meniscus velocity was calculated using the equation

$$u(l)_{i=2} = \frac{r_2^2 \Delta p_2}{8\mu\left[\lambda_1 (r_2/r_1)^4 + l - \lambda_1\right]}, \tag{3}$$

where $\Delta p_2 = 2\gamma \cos\theta / r_2$. As it is normally considered in modeling the capillary flow in tubes of nonuniform cross sections,[10–13] eqn (3) assumes the flow to quickly relax to unidirectional streamlines after the step change, and the contact angle to immediately recover the value corresponding to the straight section. These assumptions, as well as the implicit quasi-steady-state approximation, are even more suitable in mesoporous films, where both Reynolds and capillary numbers were calculated to be extremely low (Re = $\rho u_c 2r/\mu \sim 10^{-5}$ and Ca = $\mu u_c/\gamma \sim 10^{-5}$, considering water at room temperature and a relatively large characteristic velocity $u_c = 10^{-3}$ m s^{-1}).

Using the above procedure to calculate the fluid velocity over consecutive segments, up to an arbitrary position $x = l$ in the j-th step, led to the following expression for the meniscus velocity,

$$u(l)_{i=j} = \frac{\beta r_j}{l + \sum_{i=1}^{j-1} \lambda_i \left[(r_j/r_i)^4 - 1\right]}; \quad j \ge 2 \tag{4}$$

where $\beta = \gamma \cos\theta / (4\mu)$. As the experimental observations were made every few micrometers, while λ_i was on the nanometer scale,

$l \gg \lambda_i$ was satisfied from the beginning of the measurement. Further assuming the same length λ for all segments, the meniscus position can be written as $l \approx j\lambda$, and the sum in eqn (4) would be equal to $l[(r_j/r_i)^4 - 1]$. Thus, for relatively large penetration lengths, the fluid velocity in the j-th step was calculated using the equation

$$u(l)_j \approx \frac{\beta r_j}{l(r_j/r_i)^4}. \quad (5)$$

This simple expression still involves stepped variations as the meniscus advances, *i.e.*, passing through segments with different radii. Mathematically speaking, r_j and r_i may correspond to r_{max} and r_{min}, respectively or, conversely, to r_{min} and r_{max}, respectively. Although different approaches can be used to determine the average velocity of the fluid front, for the sake of simplicity, here we examined the time it took for the fluid to fill a basic periodic unit composed of two consecutive segments, that is $\tau = \Delta t_j + \Delta t_{j+1} = \lambda/u(l)_j + \lambda/u(l)_{j+1}$. Introducing eqn (5) and reordering yielded

$$\tau = \frac{l\lambda}{\beta r_{min}}\left[\left(\frac{r_{min}}{r_{max}}\right)^4 + \left(\frac{r_{max}}{r_{min}}\right)^3\right] \approx \frac{l\lambda}{\beta r_{min}}\left(\frac{r_{max}}{r_{min}}\right)^3, \quad (6)$$

provided that $l \gg \lambda$. The second equality in eqn (6) is fairly reasonable taking into account that $r_{min} < r_{max}$. It is worth noting that the same factor was recovered when averaging the function $u(l)_j$ in a periodic unit, as previously reported for sinusoidal constricted tubes.[14] Furthermore, as we were dealing with a bimodal system, eqn (6) was valid for the entire time it took for the fluid to infiltrate the entire stepped tube.[15] Actually, the prediction of eqn (6) has significant implications in filling dynamics, as discussed later. At this point, we needed to consider the physical evidence that, for a bimodal system, the radii r_i and r_j in eqn (5) correspond to, respectively, r_{min} and r_{max}. Thus, to calculate the average velocity of the fluid front, we used the expression

$$u_{av}(l) = \frac{\gamma \cos\theta}{4\mu l}\frac{{r_{min}}^4}{{r_{max}}^3} \quad (7)$$

Eqn (7) represents an average velocity, since local variations that take place in individual steps become smoothed out when $l \gg \lambda$. It is worth noting that eqn (7) still has the form $u(l) \sim 1/l$, hence the kinematic relationship $l^2 \sim t$ holds for periodically constricted tubes (PCTs). Furthermore, the dynamic coefficient for the PCT model was calculated using the equation

$$c_{PCT} = \frac{\gamma \cos\theta r_{min}}{4\mu}\left(\frac{r_{min}}{r_{max}}\right)^3 \quad (8)$$

A straightforward comparison of this equation with eqn (1) showed the effective radius of a uniform tube producing the same infiltration rate to be

$$r_{eff} = \frac{r_{min}}{(r_{max}/r_{min})^3}, \quad (9)$$

and to be always less than the smallest radius of the constricted tube (bottlenecks). This rather counterintuitive behavior is however physically consistent, and may be rationalized as follows: while the global hydrodynamic resistance is controlled by the constricted segments (r_{min}), the overall time for fluid to infiltrate the matrix is controlled by the widest pores, because fluid velocity decreases dramatically in the expanded segments. The time to fill the largest pores increases with pore volume ($\sim {r_{max}}^3$), according to eqn (6), and the infiltration rate decreases proportionally.

It is important to note that the trend predicted by eqn (9) has been experimentally observed in porous media with bimodal pore size distributions on the microscale.[15,16] In fact, the scaling ratio ${r_{min}}^4/{r_{max}}^3$ had been previously suggested from different approaches: by adding the time spent by the fluid in consecutive unit cells,[15] and from mass conservation arguments in a single step change.[16] That ${r_{min}}^4/{r_{max}}^3$ emerged in alternative calculations indicated this scaling ratio to be a key factor controlling fluid dynamics.

For the following part of the study, we used eqn (8) to interpret the results of the experiments involving capillary-driven infiltration in mesoporous films. Table 1 displays data from the study of Ceratti *et al.*,[4] but using the nomenclature of the present work. Namely, the pore sizes associated with the adsorption–desorption isotherms were considered here to be the extreme radii of the PCT model. The capillary filling experiments were carried out on a variety of mesoporous samples, using two fluids with different characteristics: water and the ionic liquid (IL) 1-ethyl-3-methylimidazolium dicyanamide. The physical properties used in our calculations included $\mu = 0.89$ mPa s and $\gamma = 71.5$ mN m^{-1} for water, and $\mu = 14.9$ mPa s and $\gamma = 44.3$ mN m^{-1} for the IL,[17] which corresponded to the temperature at which the experiments were carried out (25 °C). For the sake of clarity, $\cos\theta = 1$ was considered in both cases.

Fig. 2 shows the measured values c_{exp} (symbols) plotted as a function of the ratio ${r_{min}}^4/{r_{max}}^3$ obtained from the values of r_{min} and r_{max} listed in Table 1. Also the lines in Fig. 2 represent the prediction of eqn (8) for the physical properties of each fluid. A remarkable agreement was found between the model

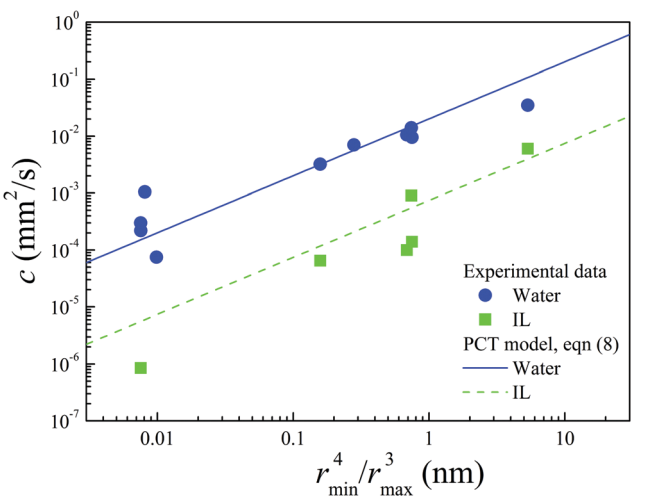

Fig. 2 Dynamic coefficient as a function of the scaling ratio for periodically constricted pores. Symbols are experimental values reported in ref. 4, and the lines are the prediction of eqn (8); the slopes $\gamma\cos\theta/(4\mu)$ were calculated using the physical properties of the respective fluids[17] (no free parameters).

and experiments, especially considering that no adjustable parameters were used in the calculations. In fact, despite a certain level of dispersion of the data, the trend predicted by the PCT model was observed over several log decades of both c_{exp} and ${r_{min}}^4/{r_{max}}^3$.

In Fig. 2, the values on the abscissa axis represent the effective capillary radius predicted by eqn (1). It is now clear that the anomalously small, physically unrealistic values of r_{eff} (less than that of an atom), and the extremely high hydrodynamic resistance levels of the mesoporous films, were due to the long time it took for the fluid to fill the pores (r_{max}) through the bottlenecks (r_{min}). In this regard, using eqn (6) provided meaningful information, by identifying the right factor controlling the infiltration rate, and showing how the infiltration time increases with pore volume ($\sim {r_{max}}^3$) for a given throat size. In the context of the PCT model, combining the meaningful nanoscale dimensions r_{max} and r_{min}, at the nanoscale, arranged as periodically varying expansions and contractions, led to a reasonable explanation of the observed infiltration dynamics.

It is worth pointing out that our PCT model compared well to previous analyses of capillary-driven flow in nonuniform tubes,[10–13] as long as relatively large penetration lengths were considered. In fact, while these reports discussed the step-like features occurring in the transitions between convergent and divergent geometries, our model focused on the dynamics over long time scales, as it addressed systems in which the length of the basic unit was negligibly small compared to the measurement length scale.

Finally, it should be mentioned that several aspects were overlooked in the modeling, such as the presence of interconnections between and bifurcations in flow paths, variations of the meniscus curvature in contractions–expansions, and the size distribution of the pores, to mention a few. Concerning this last feature, the sol–gel process has been indicated to yield pore sizes distributed around two disparate mean values, according to the bell-shaped curves obtained from adsorption–desorption isotherms.[4] This size distribution would promote a broadening of the fluid front, whose movement, however, has been shown to follow Lucas–Washburn dynamics.[18] Regarding changes in the meniscus, sharp edges and steeply changing dimensions have been suggested to lead to meniscus arrest, as well as other effects such as bubble entrapment. In the case of sinusoidal capillaries, for example, an effective contact angle for the meniscus has been described.[14,16] Relevant phenomena that may also occur are evaporation and capillary condensation, as discussed in ref. 4.

One may be tempted to conclude that these effects would play a secondary role in controlling fluid velocity, considering the effectiveness of the PCT model at representing (i) the $l^2 \sim t$ infiltration dynamics, (ii) the right magnitude of the dynamic coefficient, and (iii) its dependence on pore diameter. Of course, accounting for the physical effects discussed in the paragraph above would surely help to improve the description of the fluid flow (see examples in ref. 3). However, including additional features into the model would lead to complex formulations that would invariably require numerical simulations, where critical parameters cannot be readily identified. In contrast, the simple PCT model was based on algebraic expressions that explicitly included the key system parameters, in particular the scaling ratio ${r_{min}}^4/{r_{max}}^3$, which in our calculations appeared to capture the underlying fluid dynamics of the abnormally slow infiltration rate in mesoporous materials.

Acknowledgements

CLAB acknowledges the financial support from the Consejo Nacional de Investigaciones Científicas y Técnicas, CONICET (PIP-0363), and Universidad Nacional del Litoral, UNL (CAI + D-78-5012011010010-0), Argentina. MM acknowledges the doctoral fellowship from CNEA, Argentina.

References

1 N. Frančič, M. G. Bellino, G. J. A. A. Soler-Illia and A. Lobnik, *Analyst*, 2014, **139**, 3127–3136.
2 M. E. Calvo, N. Hidalgo, R. Schierholz, A. Kovács, A. Fernández, M. G. Bellino, G. J. A. A. Soler-Illia and H. Míguez, *Nanoscale*, 2015, **7**, 16583–16589.
3 P. Huber, *J. Phys.: Condens. Matter*, 2015, **27**, 103102.
4 D. R. Ceratti, M. Faustini, C. Sinturel, M. Vayer, V. Dahirel, M. Jardat and D. Grosso, *Nanoscale*, 2015, **7**, 5371–5382.
5 R. Lucas, *Kolloid-Z.*, 1918, **23**, 15.
6 E. W. Washburn, *Phys. Rev.*, 1921, **17**, 273–283.
7 P. G. de Gennes, F. Brochard-Wyart and D. Quére, *Capillarity and Wetting Phenomena*, Springer-Verlag, New York, 2004.
8 L. N. Acquaroli, R. Urteaga, C. L. A. Berli and R. R. Koropecki, *Langmuir*, 2011, **27**, 2067–2072.
9 R. Urteaga, L. N. Acquaroli, R. R. Koropecki, A. Santos, M. Alba, J. Pallarés, L. F. Marsal and C. L. A. Berli, *Langmuir*, 2013, **29**, 2784–2789.
10 D. Erickson, D. Li and C. B. Park, *J. Colloid Interface Sci.*, 2002, **250**, 422–430.
11 K. A. Polzin and E. Y. Choueiri, *J. Phys. D: Appl. Phys.*, 2003, **36**, 3156–3167.
12 W. Young, *Colloids Surf., A*, 2004, **234**, 123–128.
13 W. W. Liou, Y. Peng and P. E. Parker, *J. Colloid Interface Sci.*, 2009, **333**, 389–399.
14 R. Sharma and D. S. Ross, *J. Chem. Soc., Faraday Trans.*, 1991, **87**, 619–624.
15 F. A. L. Dullien, M. S. El-Sayed and V. K. Batra, *J. Colloid Interface Sci.*, 1977, **60**, 497–506.
16 D. Patro, S. Bhattacharyya and V. Jayaram, *J. Am. Ceram. Soc.*, 2007, **90**, 3040–3046.
17 E. Quijada-Maldonado, S. van der Boogaart, J. H. Lijbers, G. W. Meindersma and A. B. de Haan, *J. Chem. Thermodyn.*, 2012, **51**, 51–58.
18 S. Gruener, H. E. Hermes, B. Schillingerd, S. U. Egelhaaf and P. Huber, *Colloids Surf., A*, 2016, **496**, 13–27.

